

## PAPER

# Low-Profile Supergain Antenna Composed of Asymmetric Dipole Elements Backed by Planar Reflector for IoT Applications

Suguru KOJIMA<sup>†</sup>, Student Member, Takuji ARIMA<sup>†a)</sup>, Member, and Toru UNO<sup>†</sup>, Fellow

**SUMMARY** This paper proposes a low-profile unidirectional supergain antenna applicable to wireless communication devices such as mobile terminals, the Internet of Things and so on. The antennas used for such systems are required to be not only electrically low-profile but also unsusceptible to surrounding objects such as human body and/or electrical equipment. The proposed antenna achieves both requirements due to its supergain property using planar elements and a closely placed planar reflector. The primary antenna is an asymmetric dipole type, and consists of a monopole element mounted on an edge of a rectangular conducting plane. Both elements are placed on a dielectric substrate backed by the planar reflector. It is numerically and experimentally shown that the supergain property is achieved by optimizing the geometrical parameters of the antenna. It is also shown that the impedance characteristics can be successfully adjusted by changing the lengths of the ground plane element and the monopole element. Thus, no additional impedance matching circuit is necessary. Furthermore, it is shown that surrounding objects have insignificant impact on the antenna performance.

**key words:** *supergain, low-profile, unidirectional, asymmetric dipole antenna, planar reflector, IoT*

## 1. Introduction

In recent years, the Internet of Things (IoT) is remarkably expected as a new wireless communication service, and has been studied in various fields including antennas, microwave components and radio wave communication systems [1]–[3]. The physical size of antennas used for the IoT are highly required to be miniaturized for easily mounting on the things and to become unsusceptible to surrounding objects including the human body, as well as ensuring the stable communications as well. Thus, the antennas for the IoT are needed to be small, low-profile and to have the unidirectional property.

Several antennas have been proposed for the IoT applications [4]–[7], however, the antenna properties change quite sensitively when the antennas are placed near the human body or metallic objects when the unidirectional property has not been realized. The purpose of this paper is to develop a low-profile antenna having unidirectional property which is applicable to the mobile terminals, the IoT and so on.

Although various means are introduced in order to reduce the influence of surrounding objects on the antenna

properties [8]–[10], blocking the electromagnetic fields reflected back towards the antenna is essential in most investigations. For example, a conducting reflector is naturally used for this purpose, but a quarter wavelength ( $\lambda/4$ ) spacing between the antenna and the reflector is required. Another option is to use an Artificial Magnetic Conductor (AMC). Though the spacing can be reduced remarkably [11], the AMC completed by a mushroom-like electromagnetic band gap structure is heavy in weight and enlarges the total size of the antenna including the AMC. A relatively small and light AMC inspired antenna has been proposed [12], but a complicated substrate is required to realize the AMC behavior. Alternatively, a low-profile dipole antenna placed on a conducting plane has been investigated in which the dipole element consists of the coaxial cable itself and its unsheathed inner wire [13]. Since a 3 dB coupler and a 90-degree phase shifter must be used for feeding the antenna, this antenna is not suitable for the mobile terminals and/or the IoT devices. Other antennas such as a microstrip antenna [14] and/or a planar inverted-F antenna [15] are known to be inherently low-profile antennas with the unidirectional property, however the feed structure is complicated in general.

Since the simple structure including feed portion and parasitic elements if needed is strongly desirable for our purpose, this paper investigated the fundamental dipole antenna backed by the conducting reflector. Although a front to back ratio (F/B) can be enhanced by optimizing the size of the reflector when the distance between the half-wavelength dipole antenna and the reflector is maintained at  $\lambda/4$  [16], [17], the radiation resistance reduces to an extremely small value and then the Voltage Standing Wave Ratio (VSWR) becomes remarkably worse in general for shorter distance between the antenna and the reflector [18]. In order to overcome these difficulties, several techniques of adding a new parasitic element have been investigated [19]–[22]. In these studies, the parasitic elements are always placed in front of the feed element so that the low-profile feature is not obtained. In addition, the size of the reflector is relatively large in most cases.

Even though the above difficulties have not been resolved yet, the dipole antenna backed by the reflector remains a fundamental structure. As a consequence, this paper attempts to obtain these properties using the supergain characteristics. The antenna investigated in this paper consists of a thin planar monopole element mounted at the edge of rectangular ground plane element. This asymmetric dipole antenna is placed on a thin dielectric substrate

Manuscript received April 11, 2018.

Manuscript revised August 6, 2018.

Manuscript publicized October 15, 2018.

<sup>†</sup>The authors are with the Department of Electrical and Electronic Engineering, Tokyo University of Agriculture and Technology, Tokyo, 184-8588 Japan.

a) E-mail: t-arima@cc.tuat.ac.jp

DOI: 10.1587/transcom.2018EBP3112

backed by the planar reflector at a small distance. It is numerically and experimentally shown that the unidirectional property is achieved by optimizing the antenna geometries. It is also shown that the impedance matching can be successfully adjusted by changing the lengths of the ground plane element and/or the monopole element. Then, any additional impedance matching circuit is not necessary.

In Sect. 2, the antenna properties in free space are numerically investigated and their results are confirmed by experiments. In Sect. 3, the operating principle of the proposed antenna is clarified using the current distribution. Finally, the influences on the antenna properties from surrounding objects are investigated in Sect. 4. All of the numerical simulations were performed using a commercially provided software based on the Finite-Difference Time-Domain (FDTD) method [23].

## 2. Parameter Studies and Experimental Confirmation for Proposed Antenna

### 2.1 Antenna Configuration

Figure 1 shows the geometry of the proposed antenna. The thin monopole element is mounted on the edge of the rectangular conducting plane and fed at the base of the monopole element. Both elements make up the asymmetric dipole antenna and are placed on the 1 mm dielectric substrate that is backed by the same width and slightly long conducting reflector at the distance  $D$ . This asymmetric dipole element is considered to form a primary radiation element, therefore this paper refers it is the primary radiation element or a primary radiator simply, in order to discuss its function and the one of the reflector separately.

$L3 \times W2$  monopole element and  $L2 \times W1$  ground plane element were made by a copper foil.  $L1 \times W1$  parasitic element (reflector) was made by a thin copper plate. The total length of the reflector,  $L1$  is slightly longer than the length of the primary radiator  $L2 + L3$ . Then,  $L4$  is the distance between the edges of the dielectric substrate and the ground plane element. The relative permittivity of the substrate is 4.3 and the loss tangent ( $\tan \delta$ ) is 0.018 at 2 GHz. All

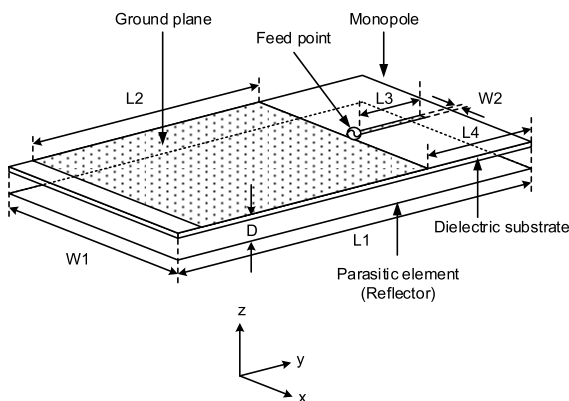


Fig. 1 Geometry of the proposed antenna.

antenna conductors are made by pure copper whose conductivity is approximately  $5.8 \times 10^7$  S/m, however in numerical calculations, they are assumed as a PEC (Perfect Electric Conductor) for simplicity. The relative permittivity and effective conductivity corresponding to the loss tangent of the substrate are assumed to be constant over a frequency range under consideration as well. The gap between the ground plane element and the monopole element is set to 1 mm.

### 2.2 Parameter Studies on Input Impedance

In this subsection, the input impedance is numerically calculated for various parameters contained in the antenna geometry. In all calculations, the frequency range is from 1.8 GHz to 2.2 GHz, and the total length of the reflector  $L1$  is set to 85 mm which is slightly longer than  $0.5 \lambda$  at the center frequency 2 GHz.

First of all, the effect of the spacing  $D$  between the primary radiator and the reflector onto the input impedance was investigated because  $D$  is an essential parameter for the low-profile property. The calculated results in which  $D$  was changed from 3 mm to 8 mm which correspond to  $0.02 \lambda$  to  $0.05 \lambda$  at 2 GHz in vacuum respectively, are shown in Fig. 2(a). The input impedance without reflector also shown in the same Smith chart. In these calculations, the other parameters were set as  $L2 = 54$  mm ( $0.36 \lambda$ ),  $L3 = 18$  mm ( $0.12 \lambda$ ),  $L4 = 25$  mm ( $0.17 \lambda$ ),  $W1 = 50$  mm ( $0.33 \lambda$ ) and  $W2 = 1$  mm, respectively. The input impedance of the antenna without reflector remains in a small region over the frequency range, however it moves toward the center of the Smith chart and a large circle was drawn by adding the reflector. It is found from these results that the reflector plays an important role in the impedance matching, and that

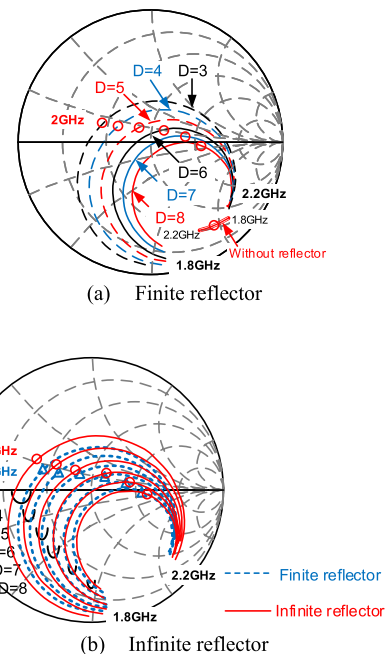


Fig. 2 Input impedance as a function of spacing  $D$ .

the antenna tends to become broadband when  $D$  becomes large within the calculated interval. Figure 2(b) shows the input impedance characteristics of an infinite reflector. The same results of Fig. 2(a) are also shown for comparison. Both frequency characteristics of the input impedances are relatively similar, but their values are considerably different from each other, especially when  $D$  is small. This indicates that the spacing  $D$  must be carefully chosen for an excellent impedance matching.

Figure 3(a) shows the effects of the width  $W1$  which is one of the important parameters related directly to the compactness of the antenna. The calculation has been performed in the interval from 30 mm to 50 mm. In this case, we set  $D = 5$  mm which correspond to  $0.03 \lambda$  at 2 GHz for simultaneously satisfying the possible low-profile property and the conclusions of Fig. 2(a) and (b). Other geometrical parameters are the same as the above case. It is found that the input impedance tends to become broadband when  $W1$  increases within the calculated range.

It has been known that the radius of the dipole antenna affects the input impedance in no small quantities. Accordingly, we check the effect of the width of monopole element  $W2$  using the same parameters as Fig. 3(a) and  $W1 = 50$  mm. The calculated results are shown in Fig. 3(b) when  $W2$  changes from 1 mm to 3 mm. It is found that the reactance component of the input impedance is reduced within the bandwidth of 280 MHz when  $W1$  decreases. Considering this result, we have decided to use  $W1 = 1$  mm monopole element hereafter.

The total length of the antenna  $L2 + L3$  is also one of the most important parameters for deciding the matching frequency. Therefore, let us separately investigate the effects of  $L2$  and  $L3$  on the input impedance. Figure 3(c) shows the input impedance when the length of ground plane element  $L2$  is changed from 52 mm to 56 mm which corresponds to  $0.35 \lambda$  to  $0.37 \lambda$  at 2 GHz under the condition that  $L3$  is 18 mm and other parameters are the same as the above case as well. It is found that the resistance and the reactance shift to the higher frequency by decreasing  $L2$ , thus the resonance frequency is able to change. Finally, the dependence of the length of monopole element  $L3$  on the input impedance are investigated. From the above discussions, we set  $L1 = 85$  mm,  $L2 = 54$  mm,  $L4 = 25$  mm,  $W1 = 50$  mm,  $W2 = 1$  mm, and  $D = 5$  mm. The calculated results are shown in Fig. 3(d). It is found that the reactance shifts from the capacitive region towards the inductive region in a lower frequency range by increasing  $L3$ , but the resistance hardly changes in the same frequency range. Thus, the impedance matching can be successfully determined by  $L2$  and  $L3$ . The resonance frequency is mainly determined by  $L2$  and its reactance value is determined by  $L3$ .

### 2.3 Experimental Confirmation

In order to confirm the validity of the numerical calculations shown above, we measured the frequency characteristics of the input impedance. The radiation patterns at the center

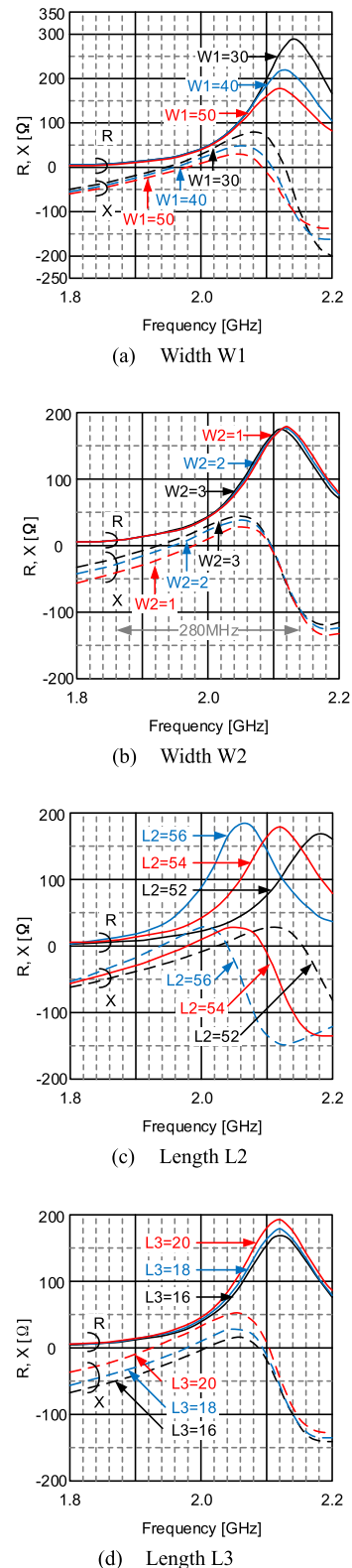


Fig. 3 Input impedance as a function of width and length.

frequency of 2 GHz are also calculated and measured in order to demonstrate that the unidirectional property can be obtained by selecting the parameters indicated above, that is,

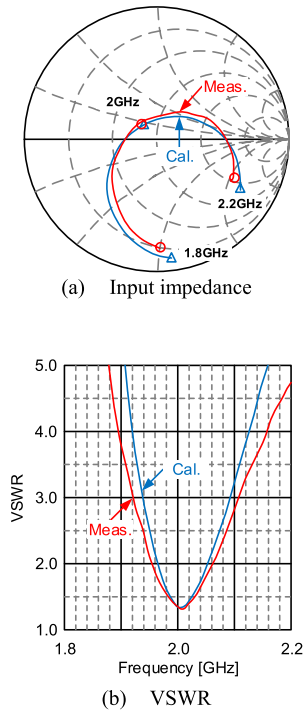


Fig. 4 Input impedance and VSWR.

$L1 = 85$  mm,  $W1 = 50$  mm,  $D = 5$  mm,  $L2 = 54$  mm,  $L3 = 18$  mm,  $L4 = 25$  mm and  $W3 = 1$  mm.

The calculated and measured frequency characteristics of the input impedance are shown in Fig. 4(a). It is shown that the measured result agrees fairly well with the calculated one. Figure 4(b) is the VSWR. It is found that the bandwidth in which the VSWR is less than 2 is about 5%.

Figure 5 shows the measured and calculated radiation patterns at 2GHz in z-x plane, z-y plane and x-y plane, respectively. Both patterns considerably agree with each other in all planes and this indicates that the unidirectional property is achieved theoretically and experimentally. It is estimated that the front to back ratio (F/B) is 20 dB and the half-value angle is about 100 degrees. The calculated gain was 7.3 dBi and the measured gain was 6.8 dBi.

### 3. Operating Principle

As numerically and experimentally demonstrated in the preceding section, the proposed antenna has the adequate unidirectional property even though the spacing between the primary radiator and the reflector is extremely small compared to the wavelength. This property predicted that the antenna may turn into the state of supergain. In order to confirm this prospect and to clarify the operation principle, we calculated the current distribution along a center line of the antenna indicated in Fig. 6(a).

Figure 6(b) shows the amplitude of a surface current density on the line which is normalized by the maximum value. The current density on the monopole element is definitely large, but almost the same degree of current can be

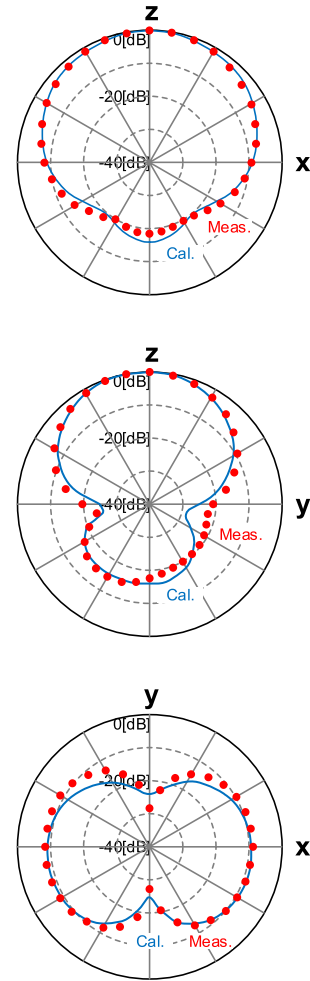


Fig. 5 Radiation patterns.

observed both on the ground plane element and the reflector in the interval of less than  $d = 60$  mm. On the other hand, Fig. 6(c) shows the phase of the current. It is found that the phase difference between the primary radiator and the reflector is approximately 180 degrees for all intervals. Thus, since the currents on the extremely closely placed conductors ( $0.03 \lambda$ ) are almost the same and the phase difference of these currents is about 180 degrees, the primary radiator turns into the state of supergain with the reflector [25], [26]. Consequently, it is considered that the unidirectional radiation is realized.

### 4. Effects of Surrounding Objects

The antenna for the IoT will be used in various situations, for example, near the human body, attached on the wireless equipment and so on. Therefore, the antenna is affected by the surrounding objects and thereby its properties may considerably change in general. However, the antenna for the IoT would be required a certain insusceptibility for stable communications. Although the proposed antenna has the unidirectional property, its property was valid in the far-field, and not demonstrated in near-field. This section investigates

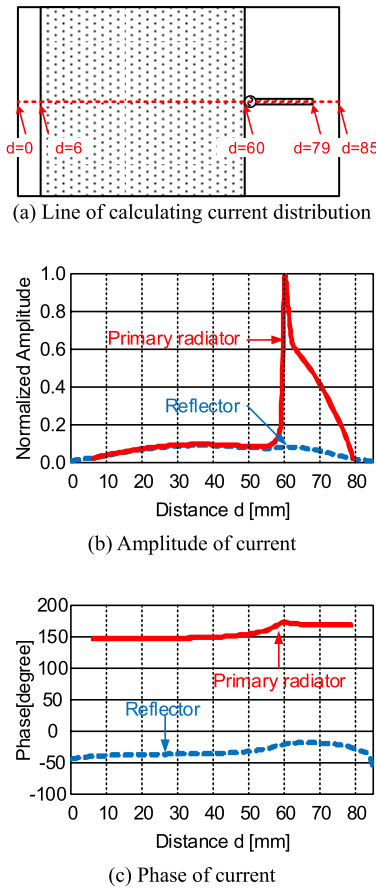


Fig. 6 Current distribution on the center line of the proposed antenna.

the effects of a nearby human head and a conducting plate on the input impedance of the proposed antenna.

4.1 Human Head

Figure 7(a) shows a geometrical arrangement of the proposed antenna placed on the temporal of human head model. The geometrical parameters of the antenna are all the same as indicated in the above section, that is,  $L1 = 85\text{ mm}$ ,  $W1 = 50\text{ mm}$ ,  $D = 5\text{ mm}$ ,  $L2 = 54\text{ mm}$ ,  $L3 = 18\text{ mm}$ ,  $L4 = 25\text{ mm}$  and  $W3 = 1\text{ mm}$ . We assumed that the human head is filled only with the brain tissue whose relative permittivity and the conductivity are  $\epsilon_r = 43.2$  and  $\sigma = 1.26\text{ S/m}$  [24], respectively.

Figure 7(b) shows the input impedance with and without the human head. A slight difference between them is observed, but both values agree considerably well with each other. This indicates that the unidirectional property indicated in Fig. 5 is maintained in the near-field, and demonstrates that interaction between the antenna and the human head is remarkably small in spite of extremely small spacing.

4.2 Conducting Plate

The influences on the antenna characteristics of the conducting object are also investigated with the assumption that

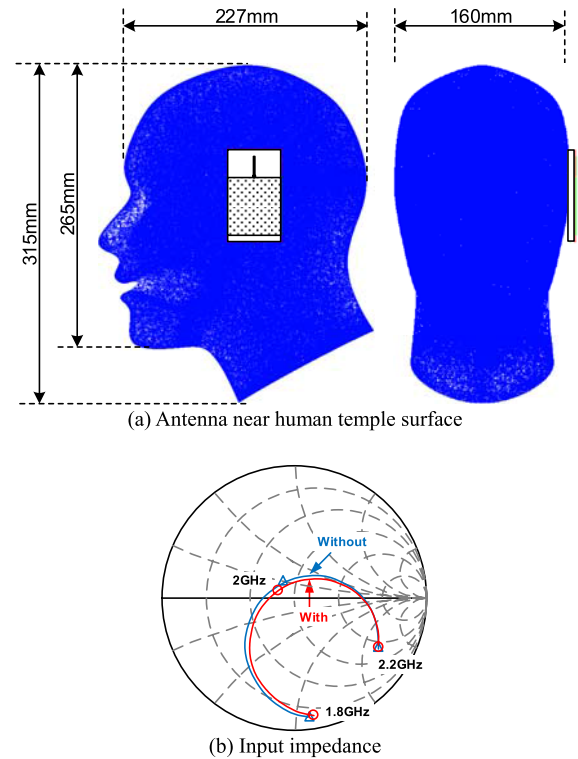


Fig. 7 Proposed antenna on the human head model.

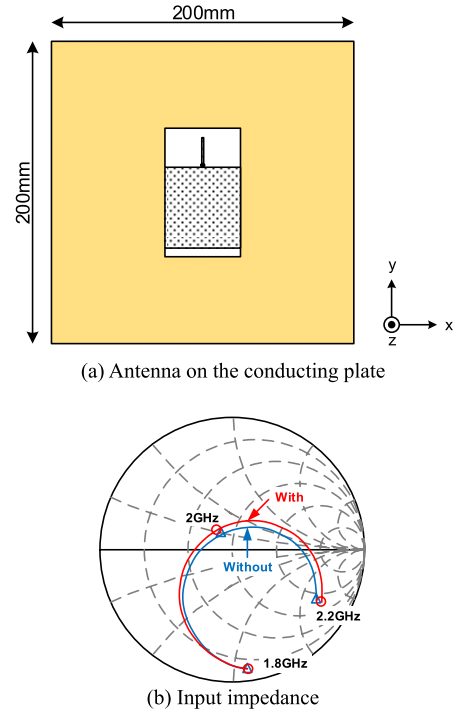


Fig. 8 Proposed antenna on the conducting plate.

the antenna is attached on the wall of electrical equipment. The geometry considered here is illustrated in Fig. 8(a) in which the antenna is placed on the surface of the  $200\text{ mm} \times 200\text{ mm}$  conducting plate. Both centers are coincident with

each other in the x-y plane.

Figure 8(b) shows the input impedances with and without the conducting plate. It is found that the influence of the closely near conducting plate on the antenna property is considerably small. Thus, the proposed antenna is hardly affected by the surrounding objects.

## 5. Conclusion

This paper has proposed a low-profile unidirectional supergain antenna mainly intended for the IoT communications. The antenna developed here is fundamentally an asymmetric planar dipole antenna backed by the reflector, and the primary part consists of the monopole element attached on the edge of the coplanar ground plane element. It has been numerically and experimentally been demonstrated that both the unidirectional property and good impedance matching performance can simultaneously be obtained by optimizing the antenna geometry even if the spacing between the primary radiation element and the reflector is very small compared to the wavelength. It has been shown by using the human head model and the large conducting plate that the antenna is hardly affected by the surrounding objects. Hence, it is expected that the proposed antenna can be successfully applied to the IoT.

## References

- [1] J. Gubbi, R. Buyya, S. Marusic, and M. Palaniswami, "Internet of Things (IoT): A vision, architectural elements, and future directions," *Future Generation Computer Systems*, vol.29, no.7, pp.1645–1660, Sept. 2013.
- [2] L.D. Xu, W. He, and S. Li, "Internet of Things in industries: A survey," *IEEE Trans. Ind. Informat.*, vol.10, no.4, pp.2233–2243, Nov. 2014.
- [3] L. Tan and N. Wang, "Future internet: The Internet of Things," *Proc. 3rd Int. Conf. Adv. Comput. Theory Eng. (ICACTE)*, vol.5, pp.376–380, Aug. 2010.
- [4] L. Lizzi, F. Ferrero, P. Monin, C. Danchesi, and S. Boudaud, "Design of miniature antennas for IoT applications," 2016 IEEE Sixth International Conference on Communications and Electronics (ICCE), pp.234–237, July 2016.
- [5] J. Jeon, K. Jang, S. Kahng, and C. Park, "Design of a miniaturized UHF-band Zigbee antenna applicable to the M2M/IoT communication," 2014 IEEE Antennas and Propagation Society International Symposium, pp.382–383, July 2014.
- [6] Y. Yang and Y. Liu, "A CPW-fed triple-band planar monopole antenna for internet of things applications," 2014 International Conference on Cyber-Enabled Distributed Computing and Knowledge Discovery, pp.380–383, Oct. 2014.
- [7] C. Chang, W. Lin, Y. Lin, and W. Liao, "Diversity antenna design for compact devices of IoT uses," 2016 IEEE International Workshop on Electromagnetics: Applications and Student Innovation Competition (iWEM), pp.1–3, 2016.
- [8] R.Y.-S. Tay, Q. Balzano, and N. Kuster, "Dipole configurations with strongly improved radiation efficiency for hand-held transceivers," *IEEE Trans. Antennas Propag.*, vol.AP-46, no.6, pp.798–806, June 1998.
- [9] K. Noguchi, M. Ando, N. Goto, M. Hirose, T. Uno, and Y. Kamimura, "Directional antenna for portable telephones," *IEICE Trans. Commun.*, vol.E79-B, no.9, pp.1234–1241, Sept. 1996.
- [10] G.F. Pedersen and J.B. Andersen, "Integrated antennas for hand-held telephones with low absorption," *Proc. 44th IEEE Veh. Technol. Conf.*, pp.1537–1541, Stockholm, Sweden, June 1994.
- [11] F. Yang and Y. Rahmat-Samii, *Electromagnetic Band Gap Structures in Antenna Engineering*, Cambridge Univ. Press, 2009.
- [12] T. Moroya, M. Kotaka, S. Makino, K. Noguchi, T. Hirota, and K. Itoh, "AMC substrate inspired small antenna MACKEY," 2015 International Symposium on Antennas and Propagation (ISAP), Hobart, TAS, Australia, Nov. 2015.
- [13] A. Thumvichit, T. Takano, and Y. Kamata, "Characteristics verification of a half-wave dipole very close to a conducting plane with excellent impedance matching," *IEEE Trans. Antennas Propag.*, vol.55, no.1, pp.53–58, Jan. 2007.
- [14] R. Garg, P. Bhartia, I. Bahl, and A. Ittipiboon, *Microstrip Antenna Design Handbook*, Artech House, UK, 2001.
- [15] K. Fujimoto and J.R. James, *Mobile Antenna Systems Handbook*, 2nd ed., Artech House, UK, 2001.
- [16] Y. Rikuta, H. Arai, and Y. Ebine, "Enhancement of FB ratio for cellular base station antenna by optimizing reflector shape," 2001 IEEE Antennas and Propagation Society International Symposium, vol.3, pp.456–459, July, 2001.
- [17] Y. Rikuta, H. Arai, and Y. Ebine, "Reflector shape optimization for FB ratio of dipole antenna," *Asia-Pacific Microwave Conference*, vol.3, pp.1068–1071, Taipei, Taiwan, June 2001.
- [18] J.D. Kraus, *Antennas*, McGraw-Hill, New York, 1988.
- [19] T. Fukasawa, H. Ohmine, K. Miyashita, and Y. Chatani, "Triple-bands broad bandwidth dipole antenna with multiple parasitic elements," *IEICE Trans. Commun.*, vol.E84-B, no.9, pp.2476–2481, Sept. 2001.
- [20] Y. Ebine and M. Ito, "A dual beam base station antenna for land mobile communications -60° beam width in horizontal plane-," *Proc. 9th Int. Conf. Antennas Propagat.*, vol.1, no.407, pp.340–343, April 1995.
- [21] M. Kijima, Y. Ebine, and Y. Yamada, "Development of a dual-frequency base station antenna for cellular mobile radios," *IEICE Trans. Commun.*, vol.E82-B, no.4, pp.636–644, April 1999.
- [22] H. Arai and K. Cho, "Cellular and PHS base station antenna systems," *IEICE Trans. Commun.*, vol.E86-B, no.3, pp.980–992, March 2003.
- [23] [http://www.engineering-eye.com/MAGNA\\_TDM/](http://www.engineering-eye.com/MAGNA_TDM/) (MAGNA/TDM Ver. 8.3, ITOCHU Techno-Solutions Corporation.)
- [24] S. Gabriel, R.W. Lau, and C. Gabriel, "The dielectric properties of biological tissues: II. Measurements in the frequency range 10 Hz to 20 GHz," *Phys. Med. Biol.*, vol.41, no.11, pp.2251–2269, Nov. 1996.
- [25] E.E. Altshuler, T.H. O'Donnel, A.D. Yaghjian, and S.R. Best, "A monopole superdirective array," *IEEE Trans. Antennas Propag.*, vol.53, no.8, pp.2653–2661, Aug. 2005.
- [26] S.R. Best, E.E. Altshuler, A.D. Yaghjian, J.M. McGinthy, and T.H. O'Donnel, "An impedance-matched 2-element superdirective array," *IEEE Antennas Wireless Propag. Lett.*, vol.7, pp.302–305, 2008.



**Suguru Kojima** received the B.S. and M.S. degrees from Tokyo University of Agriculture and Technology (TUAT), Tokyo, Japan, in 1995 and 1997, respectively. He joined Panasonic Corporation in 1997. He is currently working toward Ph.D. degree in TUAT. His research interests include the antennas for mobile terminals.



**Takuji Arima** received the M.E. and D.E. degrees in engineering from the Tokyo University of Agriculture and Technology (TUAT), Tokyo, Japan, in 1999 and 2002, respectively. He is currently an Associate Professor in the Department of Electrical and Electronics Engineering, TUAT, and also a part time Researcher at the National Institute of Information and Communications Technology, Tokyo. His research interests include computational electromagnetic and metamaterials. Dr. Arima received the Young

Scientist Award from the IEEE Antennas and Propagation Society Japan Chapter.



**Toru Uno** received the BSEE degree from Tokyo University of Agriculture and Technology (TUAT), Tokyo, Japan, in 1980, and the M.S. and Ph.D. degrees in electrical engineering from Tohoku University, Sendai, Japan, in 1982 and 1985, respectively. In 1985, he was appointed as a Research Associate in the Department of Electrical Engineering of Tohoku University, and was an Associate Professor of the same university from 1991 to 1994. He is presently a Professor in the Department of Electrical and Electronic

Engineering of the TUAT. Since August 1998 through May 1999, he was on leave from the TUAT to join the Electrical Engineering Department at the Pennsylvania State University as a Visiting Scholar. He served as chair of Technical Group on Antennas and Propagation of the Institute of Electronics, Information and Communications Engineers (IEICE) from 2011 to 2012. He also served as chair of IEEE AP-S Japan Chapter from 2005 to 2006 and an Associate Editor of IEEE Antennas and Wireless Propagation Letters from 2008 to 2013. He received the Young Scientist Award, the Distinguished Contributions Award and the Paper Award, all from the IEICE, in 1990, 2006 and 2007, respectively. His research interests include electromagnetic inverse problem, computational electromagnetics, medical and subsurface radar imagings, and electromagnetic compatibility. He is author of some books regarding the FDTD method, electromagnetic theory and antennas.